ACS Photonics

Letter

Cite This: ACS Photonics 2019, 6, 3076−3081

pubs.acs.org/journal/apchd5

Ultrafast Manipulation of a Strongly Coupled Light−Matter System by a Giant ac Stark Effect

Dmitry Panna,[†,§] Nadav Landau,[†,§] Liron Gantz,[†] Leonid Rybak,[†] Shai Tsesses,[†] Guy Adler,[†] Sebastian Brodbeck,[‡] Christian Schneider,[‡] Sven Höfling,[‡] and Alex Hayat*[,†]

[†]Department of Electrical Engineering, Technion, Haifa 32000, Israel

[‡]Technische Physik, Universität Würzburg, Am Hubland, D-97074 Würzburg, Germany

Supporting Information

ABSTRACT: We demonstrate ultrafast control of a strongly coupled light−matter system via a giant ac Stark effect in a specially designed strongly coupled microcavity using ultrafast pump−probe spectroscopy. We observe polariton energy shifts larger than the Rabi energy, enabling the implementation of strong noninvasive potentials for robust and ultrafast polaritonic switches. A nonperturbative treatment has been utilized to correctly describe the underlying physics of the giant Stark shifts in our strongly coupled light−matter system and corresponds well to the experimental results. Our findings shed new light on nonperturbative interactions and pave the way for all-optical quantum technologies.

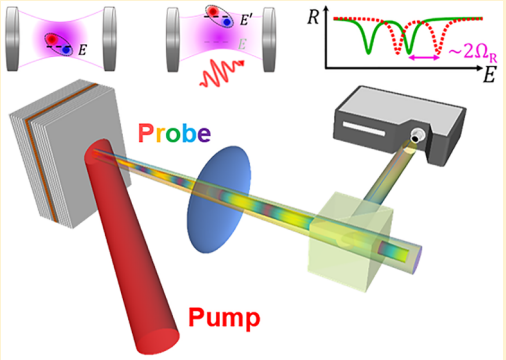

KEYWORDS: *ac Stark effect, exciton-polaritons, strong light−matter interaction, ultrafast optics, semiconductor microcavities*

Ultrafast control of matter energy levels by light is widely used through the noninvasive ac Stark effect.[1−3] Nevertheless, in strongly coupled light−matter systems, the recently observed small ac Stark shift[4] was indistinguishable from the shift of the uncoupled matter energy level. Strong light−matter coupling[5−9] imparts light properties to matter for high-temperature quantum condensation[10,11] and matter properties to light for enhanced interaction.[12−14] Specifically, strong coupling of quantum well (QW) excitons to cavity photons forms cavity exciton-polaritons[15] (Figure 1a,d) with unique optical[16] and electronic[17] properties. The hybrid light−matter nature of exciton-polaritons is manifested in very low effective mass yet relatively strong mutual interactions, which enabled observations of quantum condensation,[10,11] Bogoliubov excitations,[18] exciton-polariton lasing,[19,20] and superfluid behavior.[21−23] The ac Stark effect is utilized in various heterostructures[24−28] and two-dimensional materials[29] exhibiting excitonic resonances in order to manipulate the matter without direct carrier injection. Recently, ultrafast noninvasive control of exciton-polaritons based on the ac Stark effect was demonstrated,[4] enabling switching speeds limited only by the Stark pulse width.[30] Nevertheless, the magnitude of the Stark shift obtainable in conventional microcavity structures is limited (due to sample heating caused by pump transmission through the mirrors and its absorption in the substrate) to fractions of a millielectronvolt—an order of magnitude smaller than the typical Rabi energy. In this regime, the energy shift of the dressed polariton states cannot be distinguished from the sole shift of the exciton energy level (Figure 1b,e), as modeled by a perturbative approach. Moreover, the small shift magnitude limits potential applications, such as polariton-based switches, where large switch amplitudes ensure robustness of the logical state.

Here we demonstrate ultrafast nonperturbative control based on a giant ac Stark shift in a strongly coupled light−matter system, as observed by pump−probe differential spectroscopy (Figure 1g). We show that in the giant ac Stark effect, larger than the Rabi energy, the polariton blue shift can no longer be described as a shift of the exciton energy level only. Our experimental results reveal ultrafast nonperturbative control, which can be modeled only by full diagonalization of the underlying system Hamiltonian (Figure 1c,f). The demonstrated effects enable generation of very strong and noninvasive potentials for ultrafast manipulation of polariton condensates. Moreover, the induced shifts ensure robust operation of polariton-based switches as a result of the large switching amplitude. Our sample was grown by molecular beam epitaxy and consists of a $3\lambda/2$ AlAs intercavity layer embedded between two distributed Bragg reflector (DBR) stacks of 23 and 27 mirror pairs of $Al_{0.2}Ga_{0.8}As$/AlAs in the top and bottom DBRs, respectively. Three stacks of four 7 nm GaAs quantum wells with AlAs barriers of 4 nm width were grown at each of the three central antinodes of the microcavity to enhance the photon−exciton coupling. The main design innovation enabling our achievements lies in spectrally red-

Received: May 2, 2019
Published: November 15, 2019

DOI: 10.1021/acsphotonics.9b00659
ACS Photonics 2019, 6, 3076−3081

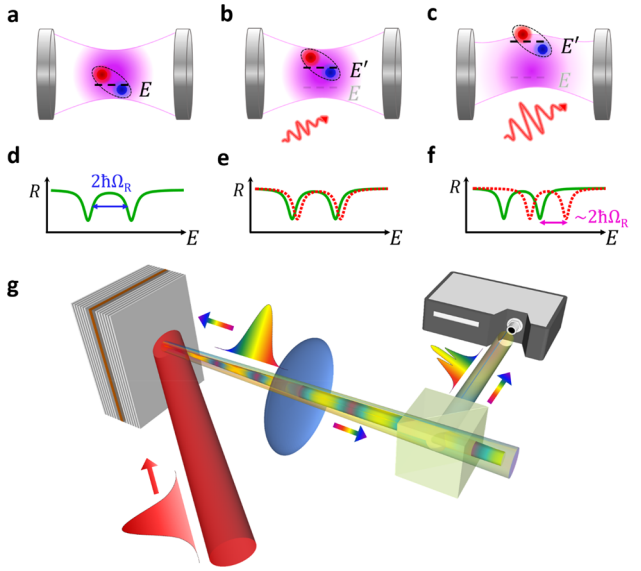

Figure 1. AC Stark shift and experimental setup. (a–c) Schematic representation of the ac Stark experiment: (a) cavity with exciton and photon (in purple) parts forming the UP and LP; (b) in the perturbative regime, for low Stark pump intensity, only the excitonic part is shifted; (c) in the nonperturbative regime, for high Stark pump intensity, the entire polariton is shifted. (d–f) Reflectivity spectra of the processes depicted in (a–c): (d) UP and LP split by twice the Rabi energy; (e) perturbative ac Stark shift (in dashed red); (f) nonperturbative ac Stark shift approaching twice the Rabi energy. (g) Experimental setup consisting of a pump beam (in red) and a supercontinuum white-light probe beam (rainbow color) impinging on the polariton microcavity. The reflected spectra are measured using a high-resolution spectrometer.

shifting the bottom DBR with respect to the top DBR by making its layers roughly 4% thicker, which creates a reflection dip in the sample spectra near 1550 meV at 45° incidence (Figure 2a). The dip was specifically designed for the Stark pump pulse, allowing it to enter the cavity at a modest angle of incidence, which is convenient for optical coupling to a cryogenic environment. The design therefore leads to reflection of the pump pulse from the bottom DBR, minimizing its absorption in the sample substrate (as can be inferred qualitatively from Figure 2c). This allows the use of high Stark pulse intensities (while exhibiting good polariton condensation) in order to realize robust all-optical polaritonic switches. The tapered DBR thickness across the sample allows tuning of the cavity resonance by probing the sample at different locations. We identified the polariton strong coupling region using reflection spectroscopy (Figure 2b). At normal incidence, a detuning energy of −9.7 meV, and a temperature of 4 K, the lower polariton (LP) and the upper polariton (UP) reflection dips were observed at 1601 and 1617 meV, respectively. The measured Rabi energy was 6.95 meV. For the chosen detuning, the LP and UP line widths were 0.8 and 2.2 meV, respectively (inset in Figure 2b), and the normalized reflectivity spectra for other detunings are depicted in Supplementary Figure 7.

First we demonstrate exciton-polariton formation and condensation in our unconventional microcavity, verifying the capability of the new device to support polariton condensates. This verification is important, because the noninvasive ultrafast manipulation of the polariton condensate utilizing the ac Stark shift could provide important applications and possible future studies using our microcavity design. Moreover, contrary to conventionally designed structures supporting the existence of polariton condensates,[4,10,11] it is not trivial to simply assume that our asymmetrically designed structure will. As mentioned, strong coupling appears in reflectivity measurements, showing polariton resonance anticrossing when the detuning tends to zero (Figure 2b), as well as in angle-resolved photoluminescence (PL) measurements showing LP dispersion, contrasting it to the bare cavity one (Figure 2d). To demonstrate condensation of the LP, we applied nonresonant pulsed laser excitation for various cavity–exciton detuning energies and injected powers at a temperature of 4K. Condensation of the LP was successfully observed at energies of 1595, 1600, and 1605 meV for detuning energies of −13.5, −7.5, and −2.9 meV, respectively (Supplementary Figures 1–6). An example of such a measurement is given in Figure 2e–g, which shows the energy, spectral width, and integrated intensity of the PL emission. These observations confirm that our specially designed microcavity structure exhibits both strong coupling of the QW exciton to the cavity photon mode and condensation of the resulting LP for various cavity–exciton detuning energies.

In our ac Stark experiment (Figure 1g), the output of a regenerative Ti:sapphire amplifier with a repetition rate of 1 kHz at 1550 meV delivering 35 fs pulses was split into two beams: one beam served as the Stark pump, and the other one generated a broad-band supercontinuum in a sapphire crystal for the probe. The probe beam, normally incident on the sample, was mildly focused in order to probe polariton states near $k_{\|} = 0$. The sample was held in a closed-cycle liquid helium cryostat at a temperature of 4 K, and its reflectivity was spectrally resolved by a high-resolution monochromator and detected with a high-sensitivity CCD camera.

The ultrafast pump pulse impinging on the sample is spectrally filtered upon being transferred through the narrow transmission dip in the semiconductor DBR mirror, resulting in a pulse spectral width of ~7.3 meV. The central pulse energy is red-detuned from the lowest polariton energy level by ~50 meV and induces nonresonant dynamic Stark shifts in the dressed states of the LP and UP without any direct excitation of the polaritons. The probability of the direct excitation is minimized for larger detuning, however, if the detuning is too large, it will adversely affect the resulting Stark shifts, as can be inferred from the derivation of the Stark effect in eq 6 in the Supporting Information. It is important to mention that the Stark pump is coupled to the excitonic part of the polariton, which is localized on the scale of tens of nanometers because of the growth nonuniformity. This localization results in a broad spread of the exciton in-plane wavenumbers on the scale of tens of reciprocal micrometers. This in turn enables the use of the normally incident probe to measure the polariton Stark shifts, whose excitonic part is coupled to the 45° incident Stark pump. This is contrary to on-resonance polariton manipulations, which require precise angle control of the pump beam.[31]

The small variation of the sample reflectivity (~3%) in the presence of the Stark pump suggests evaluating the differential reflectivity from the measured spectra to enhance the visibility of the Stark effect. A full description of the data processing is presented in the Supplementary Discussion. As shown in Figure 3a,b, our measurements clearly demonstrate the dynamic Stark blue shift of both the LP and UP lines. For increasing pump peak intensities, the shift magnitude reaches

DOI: 10.1021/acsphotonics.9b00659
ACS Photonics 2019, 6, 3076–3081

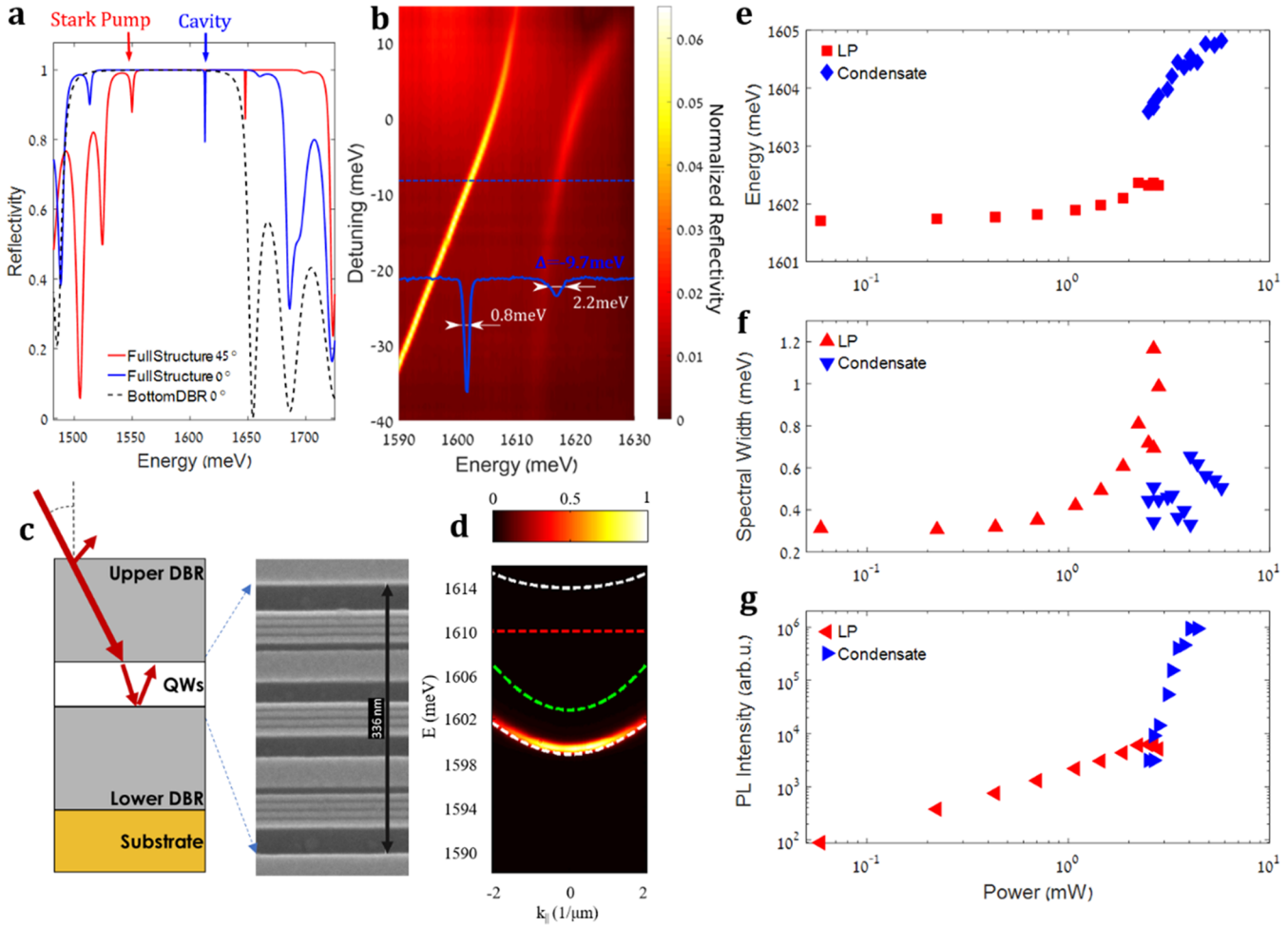

Figure 2. Sample design and polariton condensation. (a) Calculated sample reflectivities at 10 K for the full structure at normal incidence (solid blue) and at 45° incidence (solid red) and for the bottom DBR alone at normal incidence (dashed black). (b) Measured normalized reflectivity spectra of the sample at T = 4 K vs detuning (log scale), showing the Rabi splitting. The blue solid line is the normalized reflectivity spectrum at our detuning of −9.7 meV showing both the LP and UP line widths. (c) (left) Schematic drawing of the microcavity structure. The impinging and reflected pump beams are shown in red. The bottom DBR fully reflects the pump. (right) SEM image of the embedded QWs. (d) Angle-resolved photoluminescence (PL) measurement showing LP dispersion at a detuning energy of −7.5 meV and excitation power of 1.4 mW at T = 5 K. Calculated dispersions for the polaritons (dashed white), cavity photon (dashed green), and exciton (dashed red) are also shown. (e−g) Energy, spectral width, and integrated intensity of the PL emission as functions of the injection power. LP points are shown in red and condensate points in blue. These results were measured at a temperature of 4 K and a detuning of −2.9 meV between the exciton and cavity photon energies.

values larger than the vacuum Rabi energy. The Stark shifts can be extracted from the fact that each polariton experiences the maximal effect in the vicinity of zero pump−probe delay time, and blue-shifting of the polariton reflection dip to a new energy results in a differential reflectance peak at the unperturbed energy. We can safely exclude the probe beam drift on the graded sample as a possible explanation to the observed effect because the unperturbed polariton line remains vertical in the course of the experiment. The normalized differential reflectance spectra change accordingly within the extended pump pulse duration (~250 fs). For negative delay times, where the broad-band probe pulse arrives before the pump pulse, we observe coherent oscillations of the probe polarization.[32−36] These arise because the ultrafast pump perturbs the probe-induced coherent polarization within its longer decay time. When the pump−probe delay time vanishes, the spectral period of coherent oscillations diverges. In the case where the external pump is red-detuned from the polariton energies, coherent oscillations are observed together with the Stark shift of the polaritonic lines in the differential reflectivity spectra. Contrary to conventional microcavities,[4] where the spectral shifts of the polaritons are small compared with their line widths, such that the shift magnitudes determine the amplitudes of their normalized differential reflectance features, here the polariton line widths are smaller and their spectral shifts are considerably larger, so no such relation exists. When the Stark shift is smaller than the polaritonic line width, the amplitude of the normalized differential reflectivity is in fact set by the shift value. However, when the shift is larger than the polaritonic line width, the amplitude of the normalized differential reflectivity remains mostly unchanged even for larger shift values and is rather determined by the shift of the reflectivity features. Therefore, it is important to stress that extraction of the polariton Stark shifts from the amplitude of the normalized differential reflectivity (which was performed for the small shifts in ref 4) is incorrect for shifts larger than the polaritonic line width. Here the shifts were extracted from the spectral difference between the peak and dip in differential reflectivity of each polariton feature in the vicinity of zero pump−probe delay time.

DOI: 10.1021/acsphotonics.9b00659
ACS Photonics 2019, 6, 3076−3081

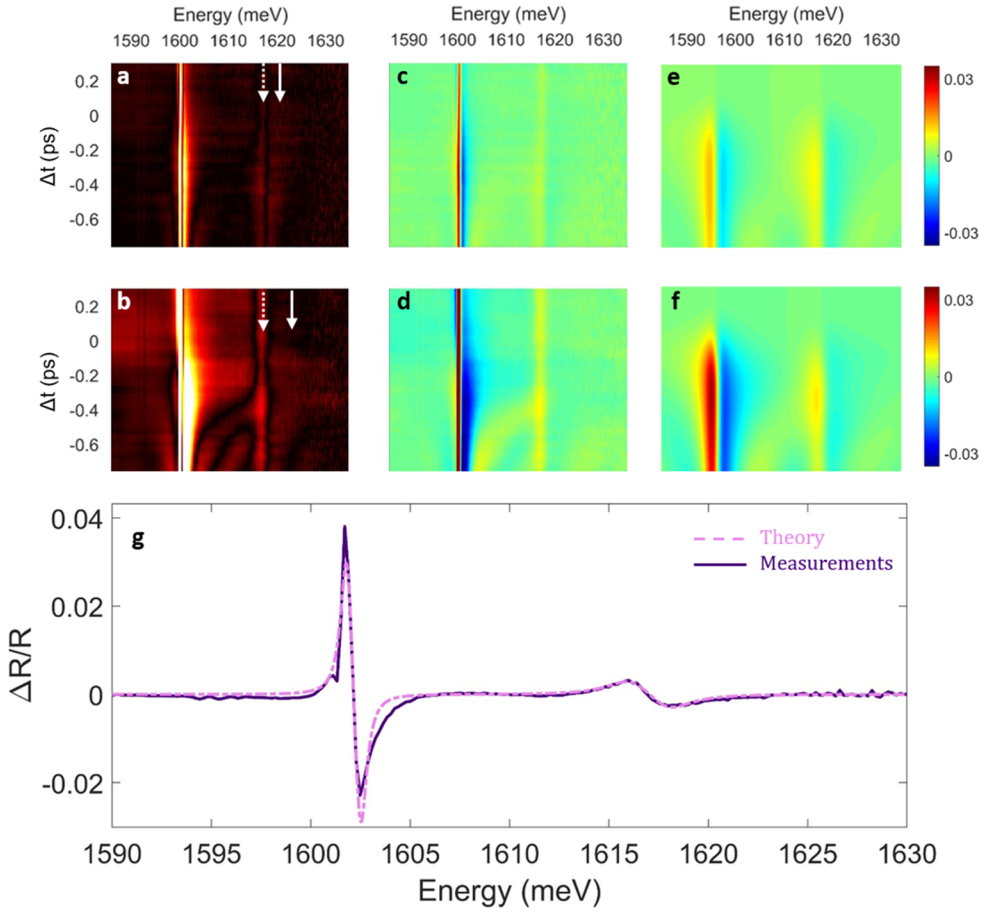

Figure 3. Normalized differential reflectivity measurements and theoretical modeling. (a, b) Measured normalized differential reflectivity on a logarithmic scale [$\log_{10}(|\Delta R/R| + 1)$] for peak intensities of 3.7 and 12.3 GW/cm^2, respectively. White arrows depict the original (dashed) and final (solid) positions of the upper polariton. (c, d) Normalized differential reflectivities $\Delta R/R$ on a linear scale for the same intensities as in (a) and (b). (e, f) Calculated normalized differential reflectivities. (g) Normalized differential reflectivity as a function of energy for near zero pump−probe delay time at a pump peak intensity of 3.7 GW/cm^2. The dashed line depicts the theoretical fit used for Stark shift magnitude extraction.

For the detuning of −9.7 meV used in our experiment, the lower polariton is more cavity-like while the upper polariton is more exciton-like. This results in larger Stark shift magnitudes for the UP with respect to the LP because the Stark pump photon interacts with the polaritons via their constituent excitonic parts. In addition, the narrower line width of the LP results in its enhanced visibility with respect to the UP feature in the normalized differential reflectivity plots in Figure 3c,d, and therefore, a logarithmic scale representation is included in Figure 3a,b to enhance the visibility of the UP feature, together with white arrows depicting the positions of the unperturbed and perturbed UP energies. The normalized differential reflectivity spectrum for a pump peak intensity of 3.7 GW/cm^2 at near-zero pump−probe delay time is shown in Figure 3g, together with the theoretical fit used to extract the Stark shift magnitude. The observed Stark shift in our specialized microcavity at high pump intensities is at least an order of magnitude higher than previously observed shifts and is also larger than the vacuum Rabi energy ($\hbar\Omega_R$ = 6.95 meV). For these pump intensities, we succeed in coupling the Stark pump strongly into the cavity and inducing extreme polariton shifts, such that the perturbative modeling in which the pump shifts the exciton energy level alone is no longer valid. In this high-intensity pump regime, correct modeling of the system requires diagonalization of the full Hamiltonian, where the photonic and excitonic parts of the polaritons are not treated separately.

Another noticeable feature appears in the normalized differential reflectivity spectra at positive times. Because of the high intensities used in the experiment, two-photon absorption generates carriers inside the semiconductor mirrors, modifying their absorption spectra and the refractive index. This in turn changes the resonance position of the cavity, resulting in a slight red shift of the polariton lines (<0.4 meV), which leaves a characteristic alternating differential reflectivity trace at positive times. However, the modification of the cavity spectra is small and, most importantly, several orders of magnitude slower than the femtosecond ac Stark effect. An additional effect present in Figure 3 is a considerable spectral broadening of both polariton dips following the blue shift, most notably of the UP, during a subpicosecond time scale roughly equivalent to our extended pump pulse duration (ruling out heating as a possible explanation for this effect). The phenomenon is enhanced for higher pump intensities and can be partially explained by the fact that our pump pulse duration was slightly shorter than the generalized exciton−cavity Rabi cycle period (~500 fs). Therefore, the Stark shift was faster than the energy exchange between the QW exciton and the cavity photon in our system, leading to the observed diabatic behavior throughout all of our measurements.

In order to explain the obtained Stark shift results theoretically, we begin with the 2 × 2 Hamiltonian for a strongly coupled light−matter system, which in our case

DOI: 10.1021/acsphotonics.9b00659
ACS Photonics 2019, 6, 3076−3081

consists of the cavity and the exciton energies, and the off-diagonal exciton−cavity interaction term. The light−matter polariton eigenenergies of the system are given by[4]

$$E_{\mathrm{LP,UP}} = \frac{1}{2}(E_{\mathrm{C}} + E_{\mathrm{X}} \pm \sqrt{4(\hbar\Omega_{\mathrm{R}})^2 + (E_{\mathrm{C}} - E_{\mathrm{X}})^2}) \quad (1)$$

where E_{X} and E_{C} are the uncoupled exciton and cavity photon energies and $\hbar\Omega_{\mathrm{R}}$ is the Rabi energy, representing the coupling between the exciton and the cavity photon. These LP and UP energies correspond to the unperturbed system without a Stark pump photon present. The ac Stark shift of such a dressed exciton-polariton system is described by adding terms representing the Stark pump−exciton interaction and the pump photon energy to the original system, expanding it to a 3 × 3 Hamiltonian of the following form:

$$H = \begin{pmatrix} E_{\mathrm{X}} & \hbar\Omega_{\mathrm{R}} & \hbar\Omega_{\mathrm{p}} \\ \hbar\Omega_{\mathrm{R}} & E_{\mathrm{C}} & 0 \\ \hbar\Omega_{\mathrm{p}} & 0 & \hbar\omega_{\mathrm{p}} \end{pmatrix} \quad (2)$$

in which $\hbar\omega_{\mathrm{p}}$ is the pump photon energy and $\Omega_{\mathrm{p}} = |\mathbf{d}\cdot\mathbf{E}_{\mathrm{p}}|/\hbar$ (where $\mathbf{d}$ is the exciton dipole matrix element and $\mathbf{E}_{\mathrm{p}}$ is the external pump electric field) is the coupling between the exciton and the external pump. For lower pump intensities and thus weaker coupling between the pump and the exciton, the blue shift can be approximated by the change in polariton energies solely due to the exciton Stark shift.[4] For higher pump intensities, however, this approximation no longer holds, and diagonalization of the full Hamiltonian is necessary. The exact analytical solution of the aforementioned Hamiltonian (see the Supplementary Discussion) leads to the UP and LP shifts as functions of the pump intensity (Figure 4). For comparison, we also plot the perturbatively calculated shift obtained using eq 7 in the Supplementary Discussion.

The calculated dependence of the shift on the pump intensity shows a considerable discrepancy of several millielectronvolts (which is significantly larger than the polariton line width) between the full and perturbative solutions for the UP, which is more exciton-like for our negatively detuned conditions. The discrepancy is even more pronounced when the Stark shift exceeds the Rabi energy, which may serve as a threshold for validity of the perturbative approach. For pump peak intensities above 13 GW/cm^2, the UP shift exceeds the Rabi energy ($\hbar\Omega_{\mathrm{R}}$ = 6.95 meV). We can further deduce that in this regime our measurements coincide well with the full solution rather than the perturbative solution. The observed discrepancy from the perturbative solution can be intuitively explained if the system composed of the exciton, pump, and cavity photons is modeled as two coupled harmonic oscillators. In this system, both the cavity and pump photons are coupled to the exciton. The strength of the coupling between the cavity photon and the exciton is determined by the Rabi frequency. In the case where the coupling of the pump photon to the exciton is much smaller than the Rabi frequency, this coupling can be considered perturbative, and the modification of the polariton energies can be fully attributed to the shifted exciton energy. This external coupling will only slightly modify the first oscillator dynamics set by the Rabi frequency. However, when the coupling to the pump photon is large, the system has to be fully diagonalized because the perturbation is on the scale of the strength of the interaction between the cavity photon and the exciton. This full diagonalization accounts for the deviation between the measured Stark shifts and the shifts predicted by the perturbative theory.

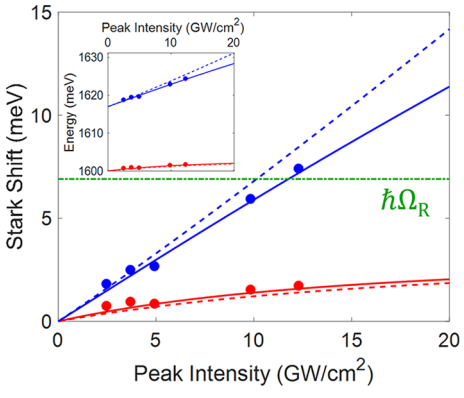

Figure 4. Magnitudes of the ac Stark shifts of the LP (red) and UP (blue) as functions of the pump peak intensity. Measured shifts are depicted by the solid circles. The calculated shifts in the full (solid lines) and perturbed (dashed lines) polariton energies were fitted using the pump coupling coefficient as a free parameter. The polariton vacuum Rabi energy ($\hbar\Omega_{\mathrm{R}}$ = 6.95 meV) is depicted by the dashed green horizontal line. The inset shows the absolute polariton energies as functions of the Stark pump peak intensity.

In conclusion, we have observed ultrafast control of a strongly coupled light−matter system based on a giant nonresonant ac Stark shift in a specially designed strongly coupled microcavity. The shift is significantly larger than the vacuum Rabi energy and thus requires full nonperturbative modeling. Our results provide new insights into light−matter interactions and enable control of the internal dynamics of the system on the femtosecond time scale, making it a strong and yet noninvasive tool for ultrafast all-optical control of quantum condensates.

■ ASSOCIATED CONTENT

Supporting Information

The Supporting Information is available free of charge at https://pubs.acs.org/doi/10.1021/acsphotonics.9b00659.

Detailed theoretical modeling, sample characterization, and data processing description (PDF)

■ AUTHOR INFORMATION

Corresponding Author

*E-mail: alex.hayat@ee.technion.ac.il.

ORCID

Shai Tsesses: 0000-0003-0167-3402

Alex Hayat: 0000-0002-6579-7431

Author Contributions

§D.P. and N.L. contributed equally to this work.

Notes

The authors declare no competing financial interest.

■ REFERENCES

(1) Shin, Y.; Saba, M.; Pasquini, T. A.; Ketterle, W.; Pritchard, D. E.; Leanhardt, A. E. Atom Interferometry with Bose−Einstein Condensates in a Double-Well Potential. *Phys. Rev. Lett.* **2004**, *92*, No. 050405.

(2) Denschlag, J.; Simsarian, J. E.; Feder, D. L.; Clark, C. W.; Collins, L. A.; Cubizolles, J.; Deng, L.; Hagley, E. W.; Helmerson, K.;

DOI: 10.1021/acsphotonics.9b00659
ACS Photonics 2019, 6, 3076−3081

Reinhardt, W. P.; Rolston, S. L.; Schneider, B. I.; Phillips, W. D. Generating Solitons by Phase Engineering of a Bose−Einstein Condensate. *Science* **2000**, *287*, 97−101.
(3) Becker, C.; Stellmer, S.; Soltan-Panahi, P.; Dörscher, S.; Baumert, M.; Richter, E. M.; Kronjäger, J.; Bongs, K.; Sengstock, K. Oscillations and interactions of dark and dark−bright solitons in Bose−Einstein condensates. *Nat. Phys.* **2008**, *4*, 496−501.
(4) Hayat, A.; Lange, C.; Rozema, L. A.; Darabi, A.; van Driel, H. M.; Steinberg, A. M.; Nelsen, B.; Snoke, D. W.; Pfeiffer, L. N.; West, K. W. Dynamic Stark effect in strongly coupled microcavity exciton-polaritons. *Phys. Rev. Lett.* **2012**, *109*, No. 033605.
(5) Thompson, R. J.; Rempe, G.; Kimble, H. J. Observation of normal-mode splitting for an atom in an optical cavity. *Phys. Rev. Lett.* **1992**, *68*, 1132−1135.
(6) Brune, M.; Schmidt-Kaler, F.; Maali, A.; Dreyer, J.; Hagley, E.; Raimond, J. M.; Haroche, S. Quantum Rabi Oscillation: A Direct Test of Field Quantization in a Cavity. *Phys. Rev. Lett.* **1996**, *76*, 1800−1803.
(7) Haroche, S. Nobel Lecture: Controlling photons in a box and exploring the quantum to classical boundary. *Rev. Mod. Phys.* **2013**, *85*, 1083−1102.
(8) Brennecke, F.; Donner, T.; Ritter, S.; Bourdel, T.; Köhl, M.; Esslinger, T. Cavity QED with a Bose−Einstein condensate. *Nature* **2007**, *450*, 268−271.
(9) Bayer, A.; Pozimski, M.; Schambeck, S.; Schuh, D.; Huber, R.; Bougeard, D.; Lange, C. Terahertz Light−Matter Interaction beyond Unity Coupling Strength. *Nano Lett.* **2017**, *17* (10), 6340−6344.
(10) Deng, H.; Weihs, G.; Santori, C.; Bloch, J.; Yamamoto, Y. Condensation of semi- conductor microcavity exciton polaritons. *Science* **2002**, *298*, 199−202.
(11) Balili, R.; Hartwell, V.; Snoke, D.; Pfeiffer, L.; West, K. Bose−Einstein Condensation of Microcavity Polaritons in a Trap. *Science* **2007**, *316*, 1007−1010.
(12) Amo, A.; Sanvitto, D.; Laussy, F. P.; Ballarini, D.; del Valle, E.; Martin, M. D.; Lemaître, A.; Bloch, J.; Krizhanovskii, D. N.; Skolnick, M. S.; Tejedor, C.; Viña, L. Collective fluid dynamics of a polariton condensate in a semiconductor microcavity. *Nature* **2009**, *457*, 291−295.
(13) Ardizzone, C.; Lewandowski, P.; Luk, M. H.; Tse, Y. C.; Kwong, N. H.; Lücke, A.; Abbarchi, M.; Baudin, E.; Galopin, E.; Bloch, J.; Lemaitre, A.; Leung, P. T.; Roussignol, P.; Binder, R.; Tignon, J.; Schumacher, S. Formation and control of Turing patterns in a coherent quantum fluid. *Sci. Rep.* **2013**, *3*, 3016.
(14) Kwong, N. H.; Tsang, C. Y.; Luk, M. H.; Tse, Y. C.; Lewandowski, P.; Chan, C. K. P.; Leung, P. T.; Schumacher, S.; Binder, R. Patterns and switching dynamics in polaritonic quantum fluids in semiconductor microcavities. *J. Opt. Soc. Am. B* **2016**, *33*, C153−C159.
(15) Weisbuch, C.; Nishioka, M.; Ishikawa, A.; Arakawa, Y. Observation of the coupled exciton-photon mode splitting in a semiconductor quantum microcavity. *Phys. Rev. Lett.* **1992**, *69*, 3314−3317.
(16) Aßmann, M.; Veit, F.; Bayer, M.; van der Poel, M.; Hvam, J. M. Higher-Order Photon Bunching in a Semiconductor Microcavity. *Science* **2009**, *325*, 297−300.
(17) Schneider, C.; Rahimi-Iman, A.; Kim, N. Y.; Fischer, J.; Savenko, I. G.; Amthor, M.; Lermer, M.; Wolf, A.; Worschech, L.; Kulakovskii, V. D.; Shelykh, I. A.; Kamp, M.; Reitzenstein, S.; Forchel, A.; Yamamoto, Y.; Höfling, S. An electrically pumped polariton laser. *Nature* **2013**, *497*, 348−352.
(18) Utsunomiya, S.; Tian, L.; Roumpos, G.; Lai, C. W.; Kumada, N.; Fujisawa, T.; Kuwata-Gonokami, M.; Löffler, A.; Höfling, S.; Forchel, A.; Yamamoto, Y. Observation of Bogoliubov excitations in exciton-polariton condensates. *Nat. Phys.* **2008**, *4*, 700−705.
(19) Tempel, J. S.; Veit, F.; Aßmann, M.; Kreilkamp, L. E.; Höfling, S.; Kamp, M.; Forchel, A.; Bayer, M. Temperature dependence of pulsed polariton lasing in a GaAs microcavity. *New J. Phys.* **2012**, *14*, No. 083014.
(20) Deng, H.; Weihs, G.; Snoke, D.; Bloch, J.; Yamamoto, Y. Polariton lasing vs. photon lasing in a semiconductor microcavity. *Proc. Natl. Acad. Sci. U. S. A.* **2003**, *100*, 15318−15323.
(21) Amo, A.; Pigeon, S.; Sanvitto, D.; Sala, V. G.; Hivet, R.; Carusotto, I.; Pisanello, F.; Leménager, G.; Houdré, R.; Giacobino, E.; Ciuti, C.; Bramati, A. Polariton Superfluids Reveal Quantum Hydrodynamic Solitons. *Science* **2011**, *332*, 1167−1170.
(22) Aßmann, M.; Tempel, J. S.; Veit, F.; Bayer, M.; Rahimi-Iman, A.; Löffler, A.; Höfling, S.; Reitzenstein, S.; Worschech, L.; Forchel, A. From polariton condensates to highly photonic quantum degenerate states of bosonic matter. *Proc. Natl. Acad. Sci. U. S. A.* **2011**, *108*, 1804−1809.
(23) Amo, A.; Lefrère, J.; Pigeon, S.; Adrados, C.; Ciuti, C.; Carusotto, I.; Houdré, R.; Giacobino, E.; Bramati, A. Superfluidity of polaritons in semiconductor microcavities. *Nat. Phys.* **2009**, *5*, 805−810.
(24) Von Lehmen, A.; Chemla, D. S.; Zucker, J. E.; Heritage, J. P. Optical Stark effect on excitons in GaAs quantum wells. *Opt. Lett.* **1986**, *11*, 609−61.
(25) Knox, W. H.; Chemla, D. S.; Miller, D. A. B.; Stark, J. B.; Schmitt-Rink, S. Femtosecond ac Stark effect in semiconductor quantum wells: Extreme low- and high-intensity limits. *Phys. Rev. Lett.* **1989**, *62*, 1189.
(26) Mysyrowicz, A.; Hulin, D.; Antonetti, A.; Migus, A.; Masselink, W. T.; Morkoç, H. "Dressed Excitons" in a Multiple-Quantum-Well Structure: Evidence for an Optical Stark Effect with Femtosecond Response Time. *Phys. Rev. Lett.* **1986**, *56*, 2748.
(27) Sieh, C.; Meier, T.; Jahnke, F.; Knorr, A.; Koch, S. W.; Brick, P.; Hübner, M.; Ell, C.; Prineas, J.; Khitrova, G.; Gibbs, H. M. Coulomb Memory Signatures in the Excitonic Optical Stark Effect. *Phys. Rev. Lett.* **1999**, *82*, 3112.
(28) Köster, N. S.; Kolata, K.; Woscholski, R.; Lange, C.; Isella, G.; Chrastina, D.; von Känel, H.; Chatterjee, S. Giant dynamical Stark shift in germanium quantum wells. *Appl. Phys. Lett.* **2011**, *98*, 161103.
(29) Sie, E. J.; McIver, J. W.; Lee, Y.; Fu, L.; Kong, J.; Gedik, N. Valley-selective optical Stark effect in monolayer WS_2. *Nat. Mater.* **2015**, *14*, 290.
(30) Cancellieri, E.; Hayat, A.; Steinberg, A. M.; Giacobino, E.; Bramati, A. Ultra-fast Stark-induced polaritonic switches. *Phys. Rev. Lett.* **2014**, *112*, No. 053601.
(31) Schumacher, S.; Kwong, N. H.; Binder, R. Influence of exciton-exciton correlations on the polarization characteristics of polariton amplification in semiconductor microcavities. *Phys. Rev. B: Condens. Matter Mater. Phys.* **2007**, *76*, 245324.
(32) Lindberg, M.; Koch, S. W. Theory of coherent transients in semiconductor pump−probe spectroscopy. *J. Opt. Soc. Am. B* **1988**, *5*, 139−146.
(33) Fluegel, B.; Peyghambarian, N.; Olbright, G.; Lindberg, M.; Koch, S. W.; Joffre, M.; Hulin, D.; Migus, A.; Antonetti, A. Femtosecond Studies of Coherent Transients in Semiconductors. *Phys. Rev. Lett.* **1987**, *59*, 2588−2591.
(34) Sokoloff, J. P.; Joffre, M.; Fluegel, B.; Hulin, D.; Lindberg, M.; Koch, S. W.; Migus, A.; Antonetti, A.; Peyghambarian, N. Transient oscillations in the vicinity of excitons and in the band of semiconductors. *Phys. Rev. B: Condens. Matter Mater. Phys.* **1988**, *38*, 7615−7621.
(35) Koch, S. W.; Peyghambarian, N.; Lindberg, M. Transient and steady-state optical nonlinearities in semiconductors. *J. Phys. C: Solid State Phys.* **1988**, *21*, 5229−5249.
(36) Lange, C.; Köster, N. S.; Chatterjee, S.; Sigg, H.; Chrastina, D.; Isella, G.; von Känel, H.; Schäfer, M.; Kira, M.; Koch, S. W. Ultrafast nonlinear optical response of photoexcited Ge/SiGe quantum wells: Evidence for a femtosecond transient population inversion. *Phys. Rev. B: Condens. Matter Mater. Phys.* **2009**, *79*, 201306.

DOI: 10.1021/acsphotonics.9b00659
ACS Photonics 2019, 6, 3076−3081